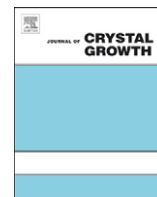




Contents lists available at ScienceDirect

Journal of Crystal Growth

journal homepage: www.elsevier.com/locate/jcrysgro

Control of active nitrogen species used for PA-MBE growth of group III nitrides on Si

Tadashi Ohachi^{a,*}, Nobuhiko Yamabe^a, Yuka Yamamoto^a, Motoi Wada^a, Osamu Ariyada^b

^a Department of Electrical Engineering, Doshisha University, Kyotanabe, Kyoto 610-0321, Japan

^b Arios Inc., Japan

ARTICLE INFO

Available online 26 November 2010

Keywords:

- A1. Molecular beam epitaxy
- A2. Plasma-assisted
- A3. Atom electrode
- B1. Nitrides

ABSTRACT

A new spiral parallel mesh electrode (PME) is presented to control active nitrogen species in plasma-assisted molecular beam epitaxial (PA-MBE) growth of group III nitrides and their alloys. Direct flux of active nitrogen from radio frequency inductive coupled plasma (rf-ICP) discharge was able to be measured using a mesh electrode for filtering charge particles and electron emission due to the self-ionization of nitrogen atoms on a negatively biased electrode. *In situ* measurement of direct nitrogen atom fluxes using the spiral PME during PA-MBE growth of GaN and AlN on Si substrates is investigated. A linear rf power dependence of direct flux of active species on atoms such as nitrogen ($N+N^*$), where N and N^* were ground and excited atoms, respectively, from a rf-ICP was confirmed by the spiral PME. An indirect flux of nitrogen adsorbed (ADS) atoms ($N+N^*$) during discharge was also monitored by the spiral PME and received influence of the wall surface of the growth chamber. ADS nitrogen atoms are able to be used for nitridation of Si surface to grow a double buffer layer (DBL) AlN/ β -Si₃N₄/Si.

© 2010 Elsevier B.V. All rights reserved.

1. Introduction

To grow group III nitride semiconductors and their alloys on large area Si substrates for energy saving materials using plasma-assisted molecular beam epitaxy (PA-MBE), the control of active nitrogen flux produced by a radio frequency inductive coupled plasma (rf-ICP) discharge of nitrogen gas is one of the key issues to be studied. Monitoring of active nitrogen atoms ($N+N^*$), which consist of ground state nitrogen atoms N and excited state nitrogen atoms N^* , is important to control the growth condition of the group III nitride compounds. A Langmuir probe has been used to measure planar, inductively coupled plasmas [1]. Wistey et al. [2] also reported on Langmuir probe for PA-MBE as an ion beam flux monitor. They used a standard ion gauge in a MBE chamber as a Langmuir probe, allowing the direct measurement of ion flux coming from a rf-ICP cell by attaching the beam flux monitor to a pico-ammeter and measuring the current impinging upon the collector or filament wires. The measured current was used to control plasma operating parameters in order to minimize the ion damage to a wafer. Real-time feedback from this measurement allows rapid optimization of the plasma for the minimum ion flux. They applied this ion beam flux to monitor the growth of GaN and dilute nitrides [2]. The present authors studied production and measurement of active nitrogen atoms ($N+N^*$) in the rf-ICP

discharge for the growth of group III nitrides and their alloys [3,4]. They measured the flux of active nitrogen atoms ($N+N^*$) instead of ion flux using a Langmuir probe-like electrode (hereafter refer to Langmuir-like probe) due to self-ionization of adsorbed (ADS) nitrogen atoms ($N+N^*$) on a negatively biased electrode, if charged particle impinging to the probe was eliminated [3]. Electron emission due to the self-ionization which emits electrons from ($N+N^*$) atoms, forms the atom current and is confirmed using different electrodes such as Pt and CuBe and different electrode area [3]. The atom current was calibrated by the grown GaN thickness grown in a VG80H MBE machine, and the calibrated flux of ($N+N^*$) atoms per atom current in the VG80H machine is 5.5×10^{-4} ML/s/nA, where ML is monolayer [3]. They reported two flux monitoring systems: one was a Langmuir-like probe to measure direct nitrogen flux from a rf-ICP cell and the other was a parallel plate electrode to measure indirect ADS nitrogen ($N+N^*$) atom flux as remote plasma irradiation [5].

A growth system of PA-MBE installing this *in situ* flux monitoring system enables realization of a single-growth process from a Si substrate to optical or electronic devices of the group III nitrides using only nitrogen gas. Indirect irradiation of nitrogen atoms was used to prepare a double buffer layer (DBL) of AlN/ β -Si₃N₄/Si with nitridation of Si substrate [6–8]. Direct irradiation of nitrogen atoms was used for the growth of AlN and GaN layers with activity modulation migration enhanced epitaxy (AM-MEE), which is one of the atomic layer epitaxial growth (ALE) processes [3].

In this report, a new spiral parallel mesh electrode (PME) is presented to control active nitrogen species such as ($N+N^*$) atoms

* Corresponding author.

E-mail address: tohachi@mail.doshisha.ac.jp (T. Ohachi).

and excited nitrogen molecules, N_2^* by measuring both direct and indirect fluxes of active nitrogen from a rf-ICP cell by self-ionization of $(N+N^*)$ atoms on a negatively biased electrode without using an eliminator for charged particles. Nitridation of Si using ADS nitrogen atoms to prepare a DBL, $AlN/\beta-Si_3N_4/Si$ is applicable to grow high-quality AlN or GaN films.

2. Experimental procedure

2.1. Rf-ICP discharge nitrogen source and in situ measuring experimental systems of direct and indirect $(N+N^*)$ fluxes

A rf-ICP cell, IRFS-501, which was made by Arios, Inc. with an automatic matching box and a time sequence controller of a rf power source, was attached to a VG80H MBE chamber as shown in Fig. 1(a) or to a measurement chamber as shown in Fig. 1(b). A spiral PME was installed in one of the shutter ports of the VG80H MBE chamber of Fig. 1(a) or was installed in the measurement chamber of Fig. 1(b). The production of $(N+N^*)$ flux and N_2^* flux was varied depending on a discharge condition at high brightness (HB) mode [5]. A strong HB discharge under high rf power and high pressure produced both higher $(N+N^*)$ atom and N_2^* molecule fluxes when

compared with a weak HB discharge power and low pressure. The LB discharge produced only N_2^* flux. Because of the long life time of $(N+N^*)$ atoms and N_2^* molecules [9] even the nitrogen mechanical shutter in the VG80H MBE chamber was closed under the HB mode; $(N+N^*)$ atoms and N_2^* molecules could be observed as indirect fluxes by leakage from the gap between the shutter and the outlet of a cell as a remote plasma condition. The HB mode is used as an ADS $(N+N^*)$ atom source with the N shutter close condition or indirect irradiation using the reflection from a wall as a remote plasma condition.

In situ measurement experiments of $(N+N^*)$ flux using spiral PME were performed in both chambers as shown in Fig. 1(a) and (b). The atom current I_A was measured using a Keithley pico-ammeter. The specifications of a PBN orifice plate were 2.0 cm diameter and 1 mm thickness with 373 holes of 0.2 mm diameter. Discharge spectra were monitored by a CCD spectrometer (Hamamatsu Photonics PMA-1) from a back port of the nitrogen cell. Optical emission intensity (OES) was a measure of the production of active nitrogen species as described elsewhere [3–5].

2.2. Parallel mesh electrode, PME

In order to monitor direct and indirect active nitrogen fluxes the self-ionization of $(N+N^*)$ atoms, as shown in Fig. 2, operated to emit electrons. A schematic self-ionization model explains the emission of electrons electrostatically, when the electrode is negatively biased. $(N+N^*)$ atoms create the atom current I_A [A] as shown in the following equation:

$$I_A = -\gamma S V_A \quad (1)$$

where γ is the self-ionization coefficient [$A/V\ m^2$], S [m^2] is the surface area of the atom electrode, and V_A [V] ($V_A = -E_A < 0$) is the atom potential at the atom electrode, which is negatively biased for self-ionization. If no charged particles come into the atom electrode, the atom current I_A corresponds to ADS $(N+N^*)$ atom flux. The minus sign comes from the negative charge of electrons. If $V_A > 0$ the current does not correspond to the atom current, because self-ionization does not occur at the electrode surface.

Fig. 3 shows an electric circuit to measure the direct atomic current through a Langmuir-like probe when no charged particles come onto the surface of the electrodes [3]. The atom current I_A of Eq. (1) depends on the atom potential V_A , which is equal to the Langmuir bias potential $V_B = -E_B$. The current I_A was the order of nA, which was measured by a Keithley pico-ammeter. When a Langmuir-like probe is a grid or filament of an ionization gauge for a flux monitor of MBE system, *in situ* measurement is not possible

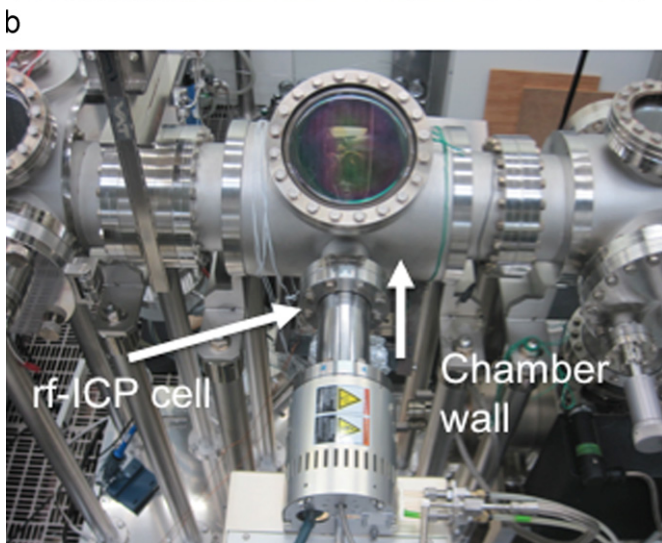
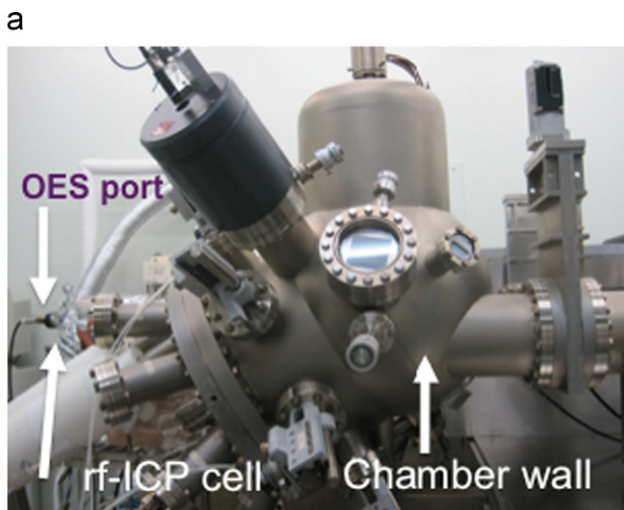


Fig. 1. Rf-ICP cell attached to a VG80H MBE chamber (a) or a measurement chamber (b).

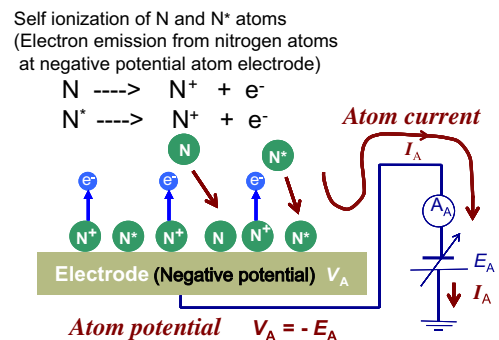


Fig. 2. Schematic self-ionization model for active nitrogen atoms from negatively biased electrode V_A , the atom potential. The atom current I_A is dependent on the surface area and V_A . The current does not correspond to the atom current if $V_A > 0$, because self-ionization does not occur on the electrode surface.

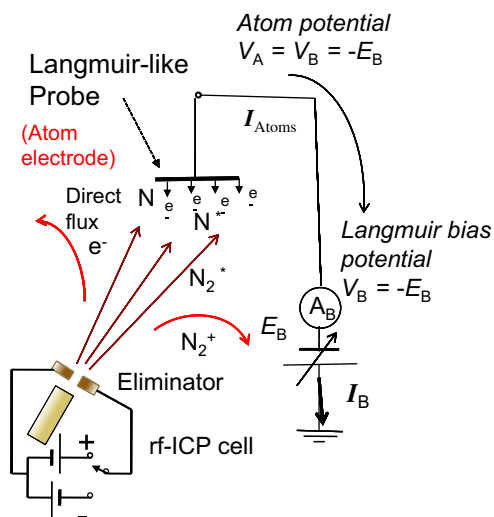


Fig. 3. Schematic drawing of a Langmuir-like probe using a grid electrode of a flux monitor installed in a V80H. The probe is biased negatively and charged particles are eliminated using an eliminator.

during the growth experiment, because the filament is placed on the back side of a sample holder.

When a PME is used as shown in Fig. 4(a) and (b), direct and indirect nitrogen ($N+N^*$) atom fluxes, respectively, are able to be measured. In the circuit, to measure direct irradiation flux, an atom electrode is defined as the electrode of the most negatively biased electrode at the position A as shown in Fig. 4(a) and (b). Both inside PME (I-PME) and outside PME (O-PME) of a spiral PME could be used as atom electrodes for the measurement of indirect irradiation flux. Only the I-PME was used as an atom electrode for the measurement of direct irradiation flux without charged particle elimination using the eliminator. In the case of Fig. 4(a), charged particles were filtered through O-PME and reached I-PME rarely. This filtering is effectively operated to eliminate charged particles impinging to I-PME without the eliminator.

When the Langmuir bias potential V_B was biased negatively, the potential of the atom potential V_A increased additionally to the potential difference between PME, E_A .

$$V_A = -E_A - E_B = -E_A + V_B. \quad (2)$$

Current, I_A is created by the self-ionization of inside surface of plate A or B. Currents, $i_{N_2}^+$ and $i_{O-N_2}^+$ are created by nitrogen molecule ions, N_2^+ coming to I-PME and O-PME, respectively. The atom currents I_A is the sum of i_A and $i_{N_2}^+$ for the configuration of Fig. 4(a) and the sum of i_A and $i_{O-N_2}^+$ for the configuration of Fig. 4(b). In the experimental settings of Fig. 4(a) and (b) during experiment, eliminator electrodes were used to control charged particle irradiation for checking the filtering effect of O-PME.

In the circuit, to measure indirect irradiation flux, both I-PME and O-PME are able to be selected as an atom electrode as mentioned above. Indirect irradiation condition is realized using shutter closing operation or placing the spiral PME in the side of nitrogen flux beam, which will be shown in the later section.

2.3. Spiral PME

Fig. 5 shows a photograph of a spiral PME, of which the dimensions of O-PME and I-PME are 50×200 and 50×150 mm², respectively, of stainless steel #100. As the spiral PME is an unsymmetrical PME, the surface area of O-PME is larger than that of I-PME. In order to separate electrically I-PME and O-PME, alumina ceramics rods are used.

In the case of direct irradiation an I-PME is selected as the atom electrode, and as shown in Fig. 4(a), the atom current between

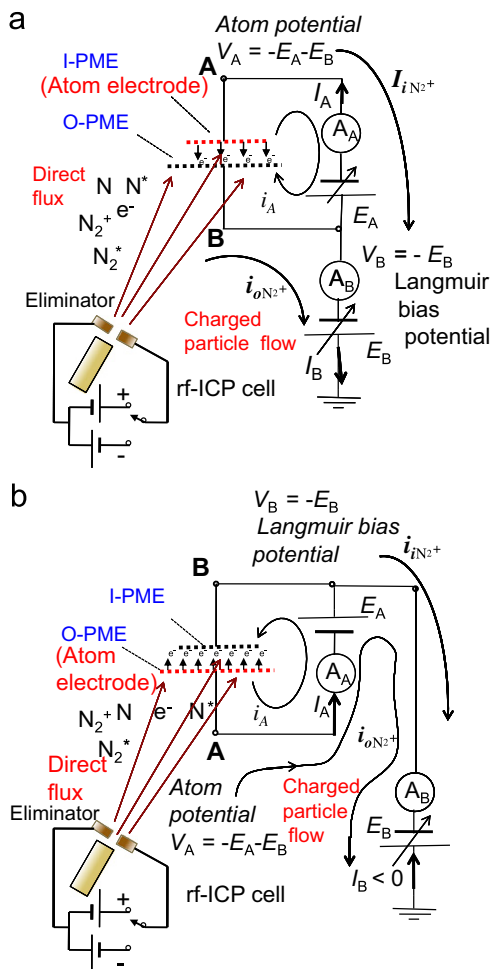


Fig. 4. (a) Direct atom current measuring configuration using I-PME as the atom PME. Charged particles are filtered through O-PME, which reach I-PME rarely. This filtering effect is effectively operated to eliminate charged particles impinging to the I-PME. This configuration was used to measure indirect atom current measurement as well. (b) This configuration, using I-PME as the Langmuir bias potential I_A , includes charged particles' current. It needs charge elimination using an eliminator like a Langmuir-like electrode. This configuration was used to measure indirect atom current measurement as well.

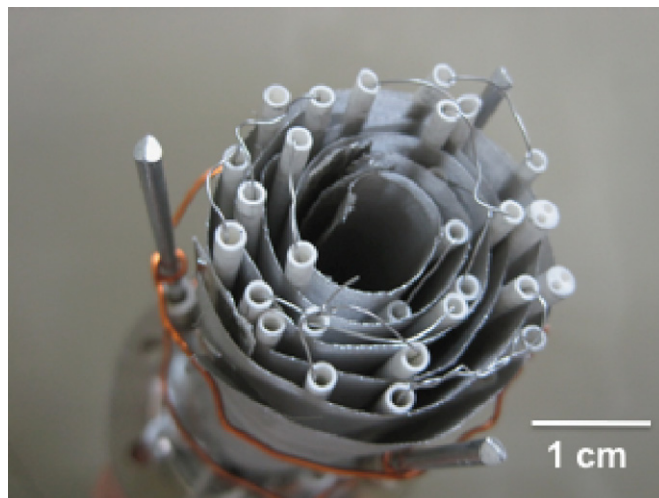


Fig. 5. Photograph of a spiral PME, which is an unsymmetrical structure. The dimensions of the outer and inner plates are 50×200 and 50×150 mm² of stainless steel #100, respectively. To separate inside and outside electrodes, alumina ceramics rods are used. This spiral PME is an unsymmetrical structure.

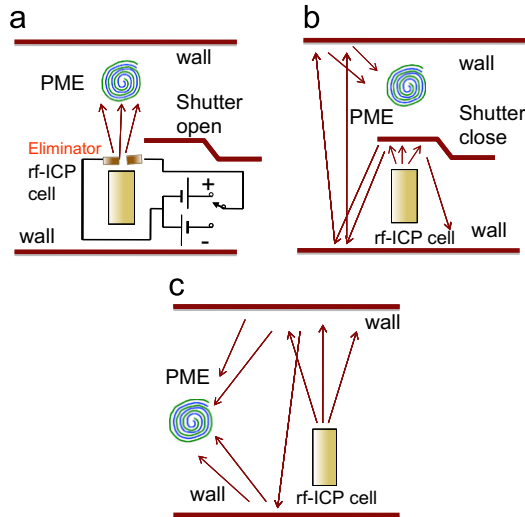


Fig. 6. *In situ* measurement of direct and indirect atom fluxes using a spiral PME. (a) Direct atom flux is formed using shutter plate open and (b) indirect atom flux is formed using shutter plate close and (c) reflection from chamber wall.

I-PME and O-PME is almost free of charged particles such as electron and N_2^+ ion fluxes. However when O-PME is selected as an atom electrode the atom current I_A includes charged particles' current. This configuration cannot be used as a monitor system for direct irradiation measurement.

In the case of indirect irradiation both I-PME and O-PME of the spiral PME can be operated as an atom electrode, which is biased at negative potential for I-PME and O-PME. The difference between the surface area of I-PME and O-PME allows the atom current difference to be calculated as in Eq. (1).

2.4. *In situ* measurement of direct and indirect $N+N^*$ fluxes

As shown in Fig. 6 *in situ* measurement of indirect and direct $N+N^*$ fluxes using a spiral PME is performed in the chamber as shown in Fig. 1(b). A shutter is placed in front of a rf-ICP cell to control flux impinging directly or indirectly to a spiral PME. An electrostatic eliminator is used to control irradiation of charged particles. Indirect ($N+N^*$) flux measurement in the VG80H growth chamber as shown in Fig. 1(a) was also performed by changing the discharge condition and shroud assembly temperatures at room temperature and at liquid nitrogen temperature.

3. Results and discussion

3.1. *In situ* measurement of direct $N+N^*$ fluxes

Constant atom current I_A over 600 V at the eliminator potential in Fig. 7 shows that the effect of charged particles did not appear due to the filtering operation of O-PME in the spiral PME. Fig. 7 shows results of direct atom flux current, I_A vs. eliminator bias potential, E_E using an experimental setup of Fig. 4(a) and (b) in a measurement chamber as shown in Fig. 1(b) and Fig. 6(a), respectively. The value difference for Fig. 4(a) and (b) comes from the difference in the surface area of the mesh electrodes of the spiral PME as shown in Fig. 5. Below 600 V for the lower eliminator potential, the effect of the charge filtering operation of O-PME was obvious. The influence of the selection of the atom electrode by a mesh electrode between the Fig. 4(a) and (b) is clearly shown in Fig. 7. The effect of charged particle filtering by O-PME of Fig. 4(a) at 0 V eliminator potential was not perfect and even a small amount of charged particle current to I-PME, $i_{N_2^+}$ is included in I_A . On the

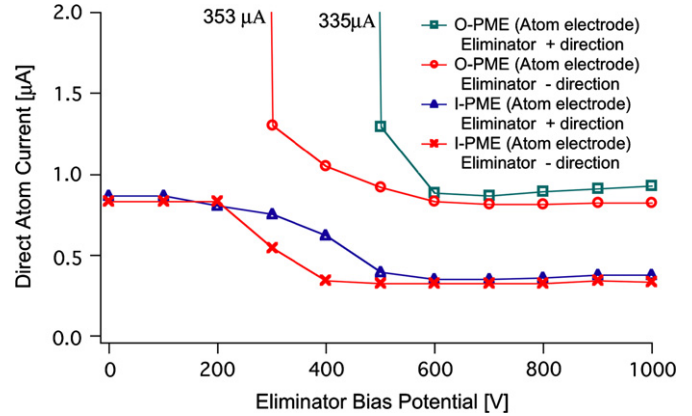


Fig. 7. Direct atom flux current vs. eliminator bias potential using an experimental setup of Fig. 4(a) and (b) using I-PME.

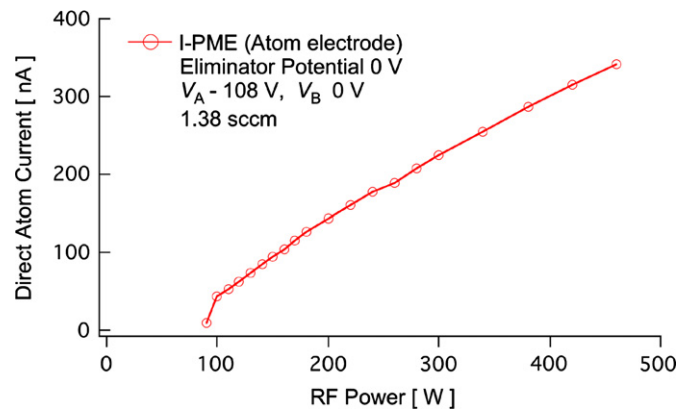


Fig. 8. Power dependence of a direct nitrogen atom flux current effused from the cell as a SS-jet flow was measured using the configuration of Fig. 4(a) without using an eliminator.

other hand I_A for a configuration of Fig. 4(b) using O-PME as the atom electrode for direct irradiation experiment confirms the additional current of charged particle current of I-PME, $i_{N_2^+}$ is very large as shown in Fig. 7.

Fig. 8 shows rf power dependence of a direct nitrogen atom flux effused from a rf-ICP cell as a SS-jet flow measured using the configuration of Fig. 4(a) without using an eliminator. This result confirms the result of the linear increase in the production of nitrogen atom ($N+N^*$) flux [3]. The small amount of charged particles' current coming to I-PME is negligibly small to be measured by the atom current, which was produced by ($N+N^*$) atom flux. The charged particle current could be reduced using an additional filtering mesh electrode placed in front of O-PME.

3.2. *In situ* measurement of indirect $N+N^*$ fluxes

Fig. 9 shows the indirect ADS atom current I_A vs. the atom potential V_A for both settings, as shown in Fig. 4(a) and (b), in a measurement chamber of Fig. 1(b). Results of Fig. 9(a) confirm that the I_A under $V_B=0$ V follows Eq. (1) when I-PME is used as the atom electrode biased in negative potential V_A . The ADS atom current I_A at $V_A = -108$ V is smaller than that of the O-PME, because the surface area ratio is proportional to $15 \times 5/20 \times 5 = 3/4 = 0.75$. The slopes of the line of negative potential range correspond to the values of γ in Eq. (1). As estimation of the surface areas of I- and O-PMEs is difficult at this moment, the value of γ is not available to be calculated. Fig. 9(b) shows increase in V_B potential to -200 V and measured I_A vs. potential difference between two PME, $V_A - V_B$. The atom potential V_A is

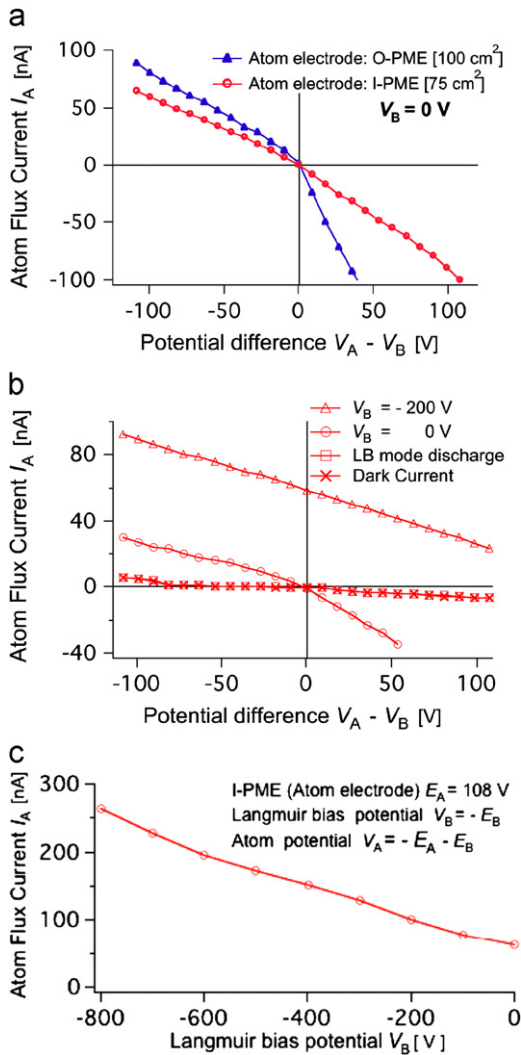


Fig. 9. Indirect ADS atom current I_A vs. potential difference between I- and O-PME, $V_A - V_B$ under 1.38 sccm nitrogen flow rate (80 P) at 500 W condition. (a) I_A for O-PME used as the atom electrode and for I-PME used as the atom electrode under $V_B = 0$ V. The effect of surface area difference of I-PME and O-PME confirms Eq. (1). (b) Shows increase in V_B potential to -200 V and measured I_A vs. $V_A + V_B$. Dark current, which is a current without discharge, and current under the LB discharge condition are also shown. Only the atom flux produces self-ionization and nitrogen atoms ($N+N^*$) are formed only in HB discharge mode and not in LB discharge mode. That is (c) shows that the indirect ADS atom flux current increases when the Langmuir potential increases with negative values. The results confirm that self-ionization of ($N+N^*$) is proportional to the atom potential V_A as given by Eq. (1).

increased by additional negative V_B values, which corresponds to -308 V for -108 V and -92 V for $+108$ V. In Fig. 9(b) dark current, which is a current without discharge, and current under the LB discharge condition are also shown. These results show that self-ionization occurred only by nitrogen ($N+N^*$) atoms formed in the HB discharge mode and not in the LB discharge mode. Fig. 9(c) shows that the indirect ADS atom flux current increases depending on V_A when the Langmuir potential increases to a negative value. The results of Fig. 9 confirm that self-ionization of ($N+N^*$) atoms is proportional to the atom potential V_A as given by Eq. (1).

3.3. Influence of wall surface on indirect $N+N^*$ fluxes

Fig. 10 shows results of *in situ* measurement of ADS nitrogen atoms using a spiral PME. When rf power was increased, the amount of active nitrogen species increased as a linear relation [3].

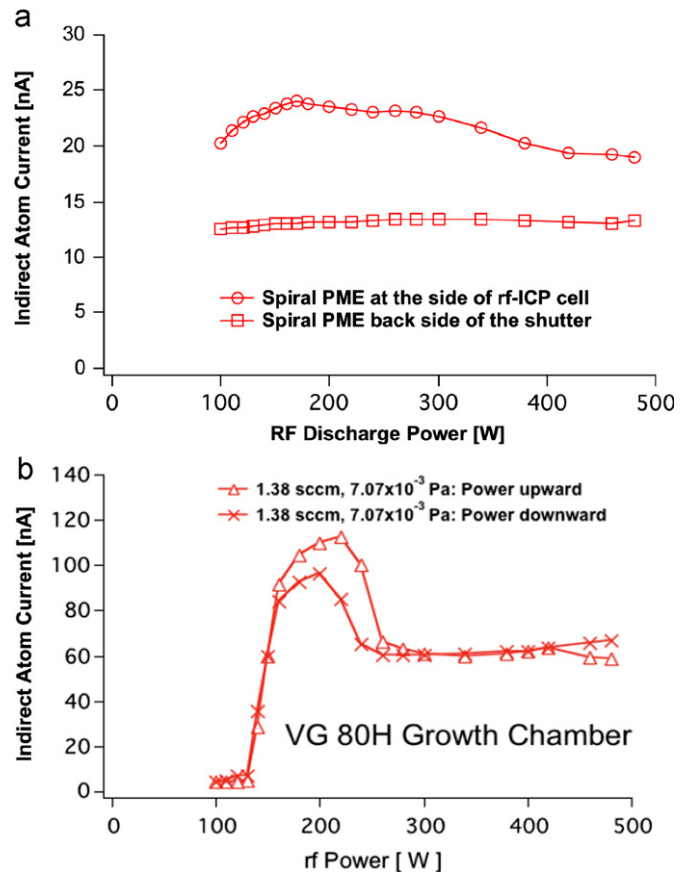


Fig. 10. Indirect ADS atom flux measurement for the chambers as shown in Fig. 1(b) and (a).

However the amount of indirect ADS nitrogen atoms did not increase linearly due to the influence of adsorption of $N+N^*$ atoms at different wall-surface conditions. The adsorption of active nitrogen species on a wall or a shutter plate in a growth chamber of Fig. 1(a) or in a measurement chamber of Fig. 1(b) affects the results of *in situ* measurement. The rf power dependence of indirect ADS atom current, which used I-PME as the atom electrodes for Fig. 6(b) and (c), gives the results of Fig. 10(a). I_A did not increase linearly even after effusing nitrogen flux was increased by rf power, as shown in Fig. 9. The indirect ADS current fluctuates and depends on the wall condition and amount of effusing atom flux, because the reflection of ($N+N^*$) atoms from the wall is changed by the condition of adsorption on the wall surface. The indirect current measured in the chamber of VG80H MBE of Fig. 1(a) at the room temperature measured by a parallel plate atom electrode is shown in Fig. 10(b). The effect of reflection from the inside wall surface of the two experimental chambers was found by the amount of the indirect atom current. The difference of inside walls in the MBE chamber and the measurement chamber is the reason for this power dependence difference in the two experimental chambers. For example an ADS nitrogen flux was changed after Al atom flux irradiation during the growth of AlN (experimental data were not shown here). *In situ* measurement of indirect ($N+N^*$) atoms is therefore very important to use ADS nitrogen atoms for nitridation of Si surfaces to produce a DBL of AlN/ β -Si₃N₄/Si [6–8].

4. Conclusions

Self-ionization of nitrogen atoms on a negatively biased electrode is demonstrated to measure *in situ* direct and indirect ($N+N^*$)

atom fluxes using a new proposed spiral PME when I-PME was used as the atom electrode. The direct flux of nitrogen ($N+N^*$) atoms from a rf-ICP increased linearly by rf power. The indirect flux of ADS ($N+N^*$) atoms during discharge as a remote plasma condition received influence from a wall of the growth chamber because of the reflected-flux reduction. *In situ* measurement of direct and indirect active nitrogen species using a spiral PME will be used to grow high-quality group III nitride semiconductors and their alloys on large area Si substrates by PA-MBE.

Acknowledgements

This work was funded by the Research Center for Interfacial Phenomena, Doshisha University. This research was partially supported by the Ministry of Education, Culture, Sports, Science, and Technology, through a Grant-in-Aid for Scientific Research B

(20360011), 2008. We are grateful to the many contributions from the students of our laboratories.

References

- [1] J. Hopwood, C.R. Guarnieri, S.J. Whitehair, J.J. Cuomo, J. Vac. Sci. Technol. A 11 (1993) 152–156.
- [2] M.A. Whistey, S.R. Bank, H.B. Yuen, J.S. Harris, M.M. Oye, A.L. Holmes Jr, J. Vac. Sci. Technol. A 23 (2005) 1.
- [3] T. Ohachi, N. Yamabe, H. Shimomura, T. Shimamura, O. Ariyada, M. Wada, J. Cryst. Growth 311 (2009) 2987.
- [4] T. Kikuchi, A.S. Somintac, O. Ariyada, M. Wada, T. Ohachi, J. Cryst. Growth 292 (2006) 221.
- [5] T. Ohachi, N. Yamabe, M. Wada O. Ariyada, Jpn. J. Appl. Phys. 50 (1), in press.
- [6] N. Yamabe, H. Shimomura, T. Shimamura, T. Ohachi, J. Cryst. Growth 311 (2009) 3049.
- [7] N. Yamabe, Y. Yamamoto, T. Ohachi, Abstract CD of ICCG-16.
- [8] Y. Yamamoto, N. Yamabe, T. Ohachi, J. Cryst. Growth, this issue.
- [9] R.P. Vaudo, J.W. Cook Jr, J.F. Schetzina, J. Vac. Sci. Technol. B 12 (1994) 1232.